Mendeleev Communications

Mendeleev Commun., 2026, **36**, 88–91

Assessment of perovskite solar cells stability under continuous illumination *via* maximum power point tracking trends analysis

Ekaterina I. Marchenko,[a,b] Natalia N. Udalova,[a] Nikolai A. Belich,[a] Pavel A. Ivlev,[a] Chengyuan Wang,[a] Yumao Li,[a] Eugene A. Goodilin[a,c] and Alexey B. Tarasov*[a,c]

[a] *Department of Materials Science, M. V. Lomonosov Moscow State University, 119991 Moscow, Russian Federation. E-mail: alexey.bor.tarasov@yandex.ru*
[b] *Department of Geology, M. V. Lomonosov Moscow State University, 119991 Moscow, Russian Federation*
[c] *Department of Chemistry, M. V. Lomonosov Moscow State University, 119991 Moscow, Russian Federation*

DOI: 10.71267/mencom.7816

The most common metric of perovskite solar cell stability, namely the time until the device loses 20% of its initial power conversion efficiency (T_{80}), was found to be oversimplified. As a much more reliable tool, a simultaneous analysis of the T_{80} and T_{50} metrics can be recommended. This makes it possible to distinguish between the stages of reversible and irreversible degradation of perovskite solar cells by the time until the device loses 20 and 50% of its initial power conversion efficiency, respectively.

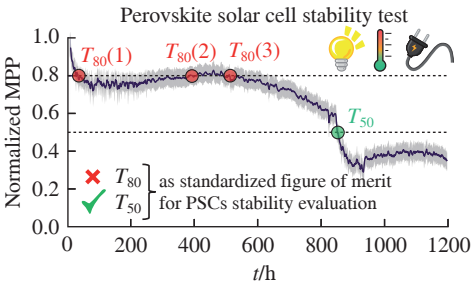

Keywords: perovskite solar cells, hybrid halide perovskites, stability, degradation trends, efficiency of devices, continuous irradiation.

Perovskite solar cells (PSCs) are a rapidly developing photovoltaic device technology that has attracted the attention of thousands of researchers worldwide.[1,2] Currently, many efforts have focused on the device stability issues, which are a key aspect for the commercialization of perovskite photovoltaics.[3–10] Various reports have shown that the stability of these devices cannot be fully assessed by standard protocols developed for conventional photovoltaic materials and devices. This requires a deeper understanding of the degradation mechanisms dominant in PSCs with the hybrid nature of the light-harvesting material.[11] While some external degradation factors such as humidity and oxygen can be mitigated by encapsulating the entire device,[12] exposure to light and heat is an inevitable and inherent condition in the operation of solar cells. This leads to the accumulation of defects in the perovskite films, causing their own degradation[13] as well as deterioration of adjacent layers,[14,15] which reduces the efficiency and stability of PSCs.[16,17] Today, one of the most common tests for PSC stability is aging under continuous irradiation with standardized solar simulators with a global horizontal irradiance spectrum (AM1.5G) and a light power density of 100 mW cm^{-2}, equivalent to 1 sun.[11] However, the interpretation of the results of such aging experiments can significantly depend on the chosen protocol for measuring the PSCs stability. Therefore, identifying proper stability metrics is a non-trivial task in perovskite photovoltaics.[18]

The time required for the efficiency to drop to 80% of the initial value is usually denoted as T_{80} and is often serves as a figure of merit for the stability of solar cells.[11] The T_{80} parameter is also considered as the minimum time for PSCs aging tests, while extrapolation of degradation curves can be used to evaluate the energy yield over the entire lifetime of solar cells.[19] At the same time, the complicated chemical origin of hybrid perovskite materials, different kinetics of interaction and migration of defects, light-induced chemical transformations and self-healing of PSCs[7,12,16,17] make it questionable to use only one criterion for an adequate description of the whole variety of interrelated processes in PSCs.

In this work, we selected 50 PSC samples with known preparation history, assembled in the same laboratory and tested exclusively under continuous 1 sun illumination by Maximum Power Point Tracking (MPPT) to analyze the stability data trends under different temperature conditions. All analyzed data were related to a series of $(MA_{0.019}Cs_{0.05}FA_{0.931})Pb(I_{0.98}Br_{0.02})_3$ perovskite† samples, which is known to have one of the most promising mixed-cation and mixed-anion compositions and is characterized by superior efficiency and relatively high stability.[20] All devices analyzed in this study were fabricated using identical protocols and have a p-i-n (inverted) architecture with the following functional layers sequence: ITO/PTAA/$(MA_{0.019}Cs_{0.05}FA_{0.931})Pb(I_{0.98}Br_{0.02})_3$/$C_{60}$/BCP/Cu/buffer layer/encapsulation glass.‡ The absolute maximum efficiency of all tested PSCs exceeded 17%. After fabrication, all devices were encapsulated according to the methodology described by Belich *et al.*[12] and subjected to long-term illumination using a full-spectrum white light source (sulfur plasma lamp set to

† The $(FA_{0.98}MA_{0.02})_{0.95}Cs_{0.05}Pb(I_{0.98}Br_{0.02})_3$ films were prepared from stoichiometric precursor solutions of formamidinium (FA) iodide, formamidinium bromide, methylammonium (MA) iodide, cesium iodide (CsI), lead bromide ($PbBr_2$) and lead iodide (PbI_2) with 30% excess of methylammonium chloride. A mixture of *N*,*N*-dimethylformamide and dimethyl sulfoxide in a volume ratio of 4 : 1 was used as a solvent. The deposition of perovskite films was carried out by a single-step spin-coating with an antisolvent (chlorobenzene) in a nitrogen-filled glove box, followed by annealing for an hour at 125 °C.

‡ ITO – indium-tin oxide transparent electrode; PTAA – poly[bis(4-phenyl)-(2,4,6-trimethylphenyl)amine] hole-conducting material; C_{60} – buckminsterfullerene electron-conducting material; BCP – bathocuproine hole-blocking material; Cu – copper electrode; MoO_3, MgF_2 or SiO_2 were used as a buffer layer for encapsulation.

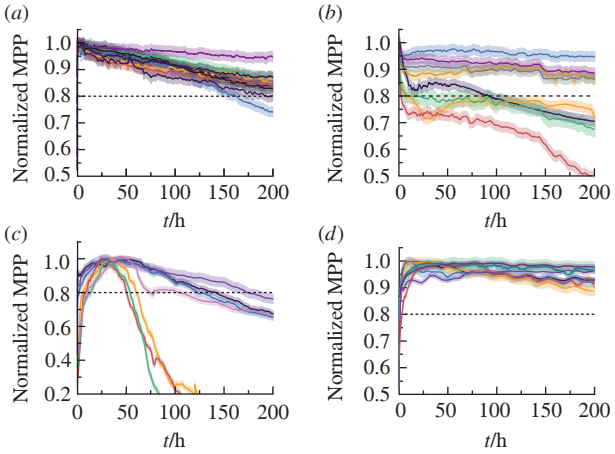

Figure 1 (*a*)–(*d*) Different PSC degradation trends under continuous 1 sun illumination at 50 °C in MPPT mode. Each curve represents the aging of an individual PSC device, demonstrating one of the many degradation trends. Different devices are shown in different colors.

100 mW cm^{-2}) with continuous MPPT at different temperatures (25, 50, 65 or 85 °C). Subsequent analysis of the obtained MPPT degradation curves revealed different types of PSC degradation behavior, despite the fact that all tested devices were nominally identical. Figure 1 illustrates four primary and most representative degradation trends observed during the first 100–200 hours of illumination at 50 °C. The first one consists of a monotonic decrease in MPP values [Figure 1(*a*)]. The second one is characterized by a rapid initial drop in efficiency during the first few hours of aging (usually referred to as the 'burn-in' process[11]), followed by a slow monotonic degradation trend [Figure 1(*b*)]. An initial sharp increase in MPP during the first few hours of the experiment, reaching a maximum value, followed by a gradual MPP decline [Figure 1(*c*)] are typical of the third degradation trend. Finally, the fourth degradation trend looks like a moderate increase in MPP during the first tens of hours, followed by a slow MPP decline [Figure 1(*d*)]. These features remain poorly understood in the scientific literature, but are generally attributed to the defect nature of the light-absorbing perovskite layer, including variations in the concentration of intrinsic defects concentration and ion losses within the devices.[21,22]

In common scientific research practice, the stability analysis of individual PSCs with record-high PCE is typically conducted over a long period of time. In contrast, primary degradation trends are more often investigated using unencapsulated devices over shorter experimental periods of 150–200 hours.[23] However, such exposure times may be insufficient to capture the full complexity of PSCs degradation behavior. Our findings indicate that in long-term stability experiments in MPPT mode, the T_{80} stability metric may not always be universally applicable. As an example, we demonstrate two devices with more than one T_{80} value on a timeline of over 500 h of MPP tracking under 1 sun illumination at 50 °C [Figure 2(*a*),(*c*)]. These T_{80} values for a single device can vary by hundreds of hours {*e.g.*, $T_{80}(1) = 98$ h, $T_{80}(2) = 105$ h, $T_{80}(3) = 430$ h and $T_{80}(4) = 515$ h [Figure 2(*a*)]}, which significantly complicates the numerical assessment of the PSC stability using the T_{80} metric. These non-monotonic changes in MPP values may correlate with different *operando* characteristics of the PSC device. For one device, a strong correlation is observed only between MPP and current density [Figure 2(*a*),(*b*)], possibly indicating the occurrence of some ionic and resistive losses.[21,22,24] For another solar cell, a similar trend in the MPPT curve during the first 700 h of aging [Figure 2(*c*)] is, on the contrary, more correlated with voltage, possibly indicating the generation and accumulation of defects inside the device. Extending the aging test beyond 700 h demonstrates similar trends for MPP, J_{MPP} and V_{MPP} characteristics [Figure 2(*d*)], which originates from a more complex and possibly irreversible degradation of the PSC on a timescale of >700 h. In this case, the T_{50} metric provides an unambiguous assessment of the PSC stability [Figure 2(*c*), green dot], unlike the T_{80} metric.

All these effects can be either reversible or irreversible due to the presence of mobile ions in metal halide perovskites and their diffusion and drift within the entire device, leading to multiple T_{80} values over time. For example, Kim *et al.*[25] proposed that iodide ions in the lattice are oxidized by photogenerated holes, resulting in the formation of neutral iodine interstitials (I_i^x) and iodide vacancies ($V_I^{\bullet}$). This process is described in defect notation as $I_i^x + h^{\bullet} \rightarrow I_I^x + V_I^{\bullet}$.

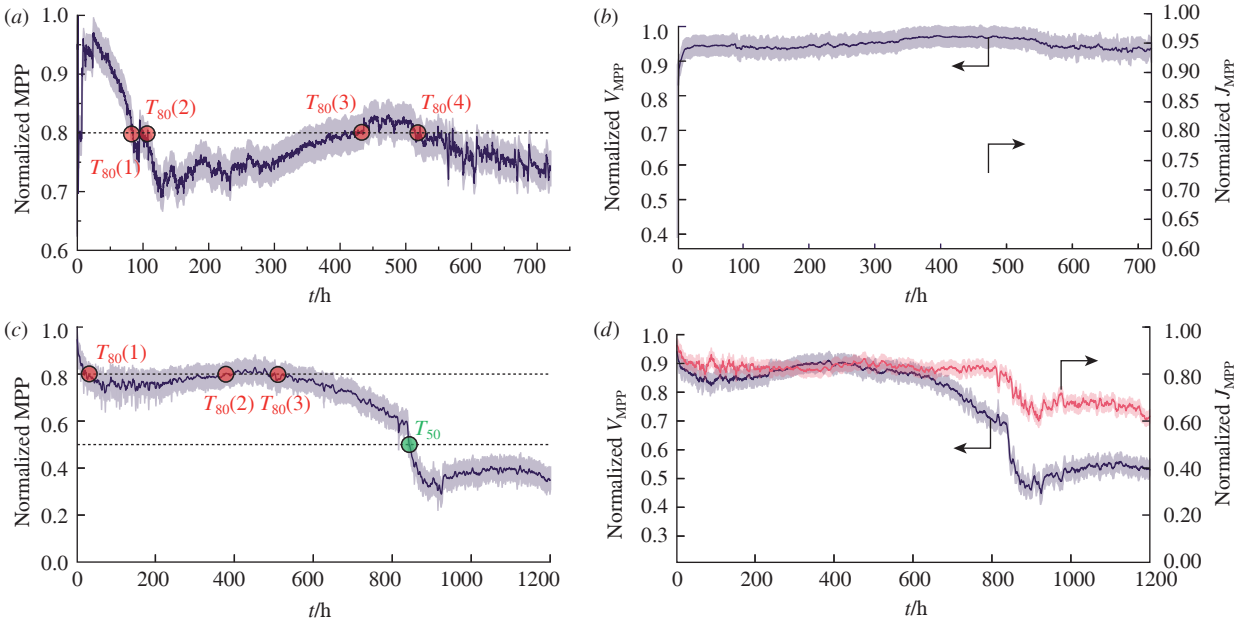

Figure 2 Using T_{80} and T_{50} metrics to evaluate the stability of two encapsulated PSCs for (*a*),(*b*) sample 1 and (*c*),(*d*) sample 2, each consisting of two separate devices, in terms of the evolution of (*a*),(*c*) MPP and (*b*),(*d*) current density (J_{MPP}) and voltage (V_{MPP}). The samples were tested under continuous 1 sun illumination at 50 °C. The shaded area represents the standard deviation for each sample between two separate pixels. All curves are normalized to the maximum.

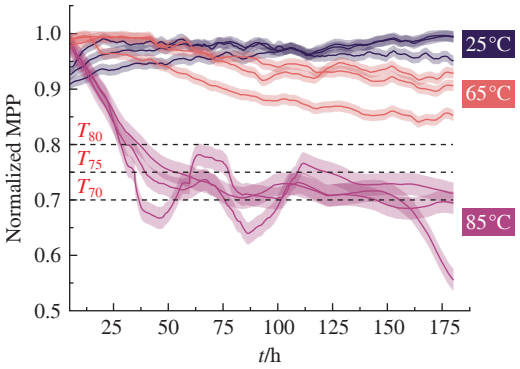

Figure 3 Degradation trends of PSCs devices at 25 °C according to the ISOS-L-1 protocol and at 65 and 85 °C according to the ISOS-L-2 protocol. Shaded areas represent the standard deviation for each curve.

At long exposure times (>700 h), additional irreversible degradation mechanisms may become significant [see Figure 2(*c*)]. For example, migration of I^0 or I^- through the device layers to the metal electrodes[26] may cause irreversible degradation of the electrodes *via* halogenation reactions (*e.g.*, Cu + I^0 → CuI).[14,27]

In contrast to the T_{80} time, which most likely depends to a greater extent on the reversible processes of perovskite degradation, the T_{50} and T_{20} metrics are determined mainly by irreversible degradation processes and therefore provide a more accurate stability assessment of PSCs.

Next, we compared the stability trends of the PSC devices at different aging test temperatures. As shown in Figure 3, for samples with the same architecture, functional layers and device fabrication protocol, the slope of the degradation trends during MPPT under continuous 1 sun irradiation depends on the temperature. For devices tested at 25 and 65 °C, the T_{80} time was not reached after more than 170 h of aging, while for devices tested at 85 °C, the T_{80} time was significantly reduced to about 26–37 h (see Figure 3). Additionally, for devices tested at 85 °C, multiple T_{75} and T_{70} points were observed during the experiment, indicating the occurrence of reversible degradation processes.

Therefore, to accurately assess the stability of PSCs, we propose to simultaneously determine the T_{80} and T_{50} (or T_{20}) values for each device under constant 1 sun irradiation at 85 °C. This approach allows us to estimate the duration of perovskite solar cells operation in the reversible degradation mode and the point at which the device enters the irreversible degradation mode with an efficiency loss of >50% (T_{50} metric). This approach is demonstrated in Table 1 for samples 1 and 2 [see Figure 2(*a*),(*c*)]. Given the multiple T_{80} metric values, we assume that both samples undergo the reversible degradation stage within 417–475 h. After this time, the MPP curve of sample 2 starts to irreversibly decline, reaching T_{50} at 845 h from the start of the aging test. The time interval between 500 and 845 h of aging sample 2 could be called a transition mode, which is most likely characterized by the accumulation of defects in the device to a critical concentration with a drop in V_{MPP}, leading to the appearance of resistive ion losses with an additional drop in J_{MPP} [see Figure 2(*d*)].

In summary, we show that the diversity of MPPT aging curve behavior of PSCs makes their stability assessment highly dependent on the choice of metric. Due to the complicated chemical nature of hybrid halide perovskites and their self-healing ability, the most common stability metric T_{80} is often ambiguous, showing multiple T_{80} values for a single device. We propose to interpret such non-monotonic MPP dynamics around 20% efficiency loss as a reversible stage of PSCs degradation. In turn, the transition to the irreversible stage of degradation is proposed to be estimated by T_{50} time. For a more informative and accurate assessment of PSCs stability, accelerated aging tests under continuous 1 sun irradiation at elevated temperatures (85 °C) should be performed according to the ISOS-L-2 protocol.

Table 1 Numerical estimation of PSC stability using the T_{80} and T_{50} metrics.[a]

Sample no.	Reversible degradation			T_{50} to irreversible degradation onset time/h
	$T_{80}(1)$/h	$T_{80}(i)$/h	$T_{80}(1)$ to $T_{80}(i)$ time/h	
1	98	515	417	>>700
2	25	500	475	845

[a] Aging conditions: 1 sun illumination, MPPT, 50 °C.

This work was supported by the Russian Science Foundation (grant no. 24-73-00308).

References

1 P. Čulík, K. Brooks, C. Momblona, M. Adams, S. Kinge, F. Maréchal, P. J. Dyson and M. K. Nazeeruddin, *ACS Energy Lett.*, 2022, **7**, 3039; https://doi.org/10.1021/acsenergylett.2c01728.
2 M. De Bastiani, V. Larini, R. Montecucco and G. Grancini, *Energy Environ. Sci.*, 2023, **16**, 421; https://doi.org/10.1039/d2ee03136a.
3 Z. Song, A. Abate, S. C. Watthage, G. K. Liyanage, A. B. Phillips, U. Steiner, M. Graetzel and M. J. Heben, *Adv. Energy Mater.*, 2016, **6**, 1600846; https://doi.org/10.1002/aenm.201600846.
4 N. Aristidou, I. Sanchez-Molina, T. Chotchuangchutchaval, M. Brown, L. Martinez, T. Rath and S. A. Haque, *Angew. Chem., Int. Ed.*, 2015, **54**, 8208; https://doi.org/10.1002/anie.201503153.
5 F. Lang, O. Shargaieva, V. V. Brus, H. C. Neitzert, J. Rappich and N. H. Nickel, *Adv. Mater.*, 2018, **30**, 1702905; https://doi.org/10.1002/adma.201702905.
6 N.-K. Kim, Y. H. Min, S. Noh, E. Cho, G. Jeong, M. Joo, S.-W. Ahn, J. S. Lee, S. Kim, K. Ihm, H. Ahn, Y. Kang, H.-S. Lee and D. Kim, *Sci. Rep.*, 2017, **7**, 4645; https://doi.org/10.1038/s41598-017-04690-w.
7 N. N. Udalova, S. A. Fateev, E. M. Nemygina, A. Zanetta, G. Grancini, E. A. Goodilin and A. B. Tarasov, *ACS Appl. Mater. Interfaces*, 2022, **14**, 961; https://doi.org/10.1021/acsami.1c20043.
8 N. N. Udalova, A. A. Petrov, E. M. Nemygina, K. R. Plukchi, E. A. Goodilin and A. B. Tarasov, *Mendeleev Commun.*, 2024, **34**, 840; https://doi.org/10.1016/j.mencom.2024.10.023.
9 E. M. Nemygina, N. N. Udalova, E. I. Marchenko, A. K. Moskalenko, E. A. Goodilin and A. B. Tarasov, *Mendeleev Commun.*, 2024, **34**, 660; https://doi.org/10.1016/j.mencom.2024.09.011.
10 N. N. Udalova, E. M. Nemygina, A. A. Petrov, E. I. Marchenko, E. S. Ibragimov, A. O. Belyaeva, A. S. Tutantsev, N. A. Belich, P. A. Ivlev, E. A. Goodilin and A. B. Tarasov, *ACS Appl. Energy Mater.*, 2025, **8**, 2239; https://doi.org/10.1021/acsaem.4c02820.
11 M. V. Khenkin, E. A. Katz, A. Abate, G. Bardizza, J. J. Berry, C. Brabec, F. Brunetti, V. Bulović, Q. Burlingame, A. Di Carlo, R. Cheacharoen, Y.-B. Cheng, A. Colsmann, S. Cros, K. Domanski, M. Dusza, C. J. Fell, S. R. Forrest, Y. Galagan, D. Di Girolamo, M. Grätzel, A. Hagfeldt, E. von Hauff, H. Hoppe, J. Kettle, H. Köbler, M. S. Leite, S. (F.) Liu, Y.-L. Loo, J. M. Luther, C.-Q. Ma, M. Madsen, M. Manceau, M. Matheron, M. McGehee, R. Meitzner, M. K. Nazeeruddin, A. F. Nogueira, Ç. Odabaşı, A. Osherov, N.-G. Park, M. O. Reese, F. De Rossi, M. Saliba, U. S. Schubert, H. J. Snaith, S. D. Stranks, W. Tress, P. A. Troshin, V. Turkovic, S. Veenstra, I. Visoly-Fisher, A. Walsh, T. Watson, H. Xie, R. Yıldırım, S. M. Zakeeruddin, K. Zhu and M. Lira-Cantu, *Nat. Energy*, 2020, **5**, 35; https://doi.org/10.1038/s41560-019-0529-5.
12 N. A. Belich, A. A. Petrov, P. A. Ivlev, N. N. Udalova, A. A. Pustovalova, E. A. Goodilin and A. B. Tarasov, *J. Energy Chem.*, 2023, **78**, 246; https://doi.org/10.1016/j.jechem.2022.12.010.
13 N. N. Udalova, A. S. Tutantsev, Q. Chen, A. Kraskov, E. A. Goodilin and A. B. Tarasov, *ACS Appl. Mater. Interfaces*, 2020, **12**, 12755; https://doi.org/10.1021/acsami.9b21689.
14 N. N. Udalova, E. M. Nemygina, E. A. Zharenova, A. S. Tutantsev, A. A. Sudakov, A. Yu. Grishko, N. A. Belich, E. A. Goodilin and A. B. Tarasov, *J. Phys. Chem. C*, 2020, **124**, 24601; https://doi.org/10.1021/acs.jpcc.0c06608.
15 N. N. Shlenskaya, N. A. Belich, M. Grätzel, E. A. Goodilin and A. B. Tarasov, *J. Mater. Chem. A*, 2018, **6**, 1780; https://doi.org/10.1039/C7TA10217H.
16 Z. Ni, H. Jiao, C. Fei, H. Gu, S. Xu, Z. Yu, G. Yang, Y. Deng, Q. Jiang, Y. Liu, Y. Yan and J. Huang, *Nat. Energy*, 2022, **7**, 65: https://doi.org/10.1038/s41560-021-00949-9.

17 J. Hieulle, A. Krishna, A. Boziki, J.-N. Audinot, M. U. Farooq, J. Ferreira Machado, M. Mladenović, H. Phirke, A. Singh, T. Wirtz, A. Tkatchenko, M. Graetzel, A. Hagfeldt and A. Redinger, *Energy Environ. Sci.*, 2024, **17**, 284; https://doi.org/10.1039/d3ee03511e.
18 P. Graniero, M. Khenkin, H. Köbler, N. T. P. Hartono, R. Schlatmann, A. Abate, E. Unger, T. J. Jacobsson and C. Ulbrich, *Frontiers in Energy Research*, 2023, **11**, 1118654; https://doi.org/10.3389/fenrg.2023.1118654.
19 R. Roesch, T. Faber, E. von Hauff, T. M. Brown, M. Lira-Cantu and H. Hoppe, *Adv. Energy Mater.*, 2015, **5**, 1501407; https://doi.org/10.1002/aenm.201501407.
20 G. Li, Z. Su, L. Canil, D. Hughes, M. H. Aldamasy, J. Dagar, S. Trofimov, L. Wang, W. Zuo, J. J. Jerónimo-Rendon, M. M. Byranvand, C. Wang, R. Zhu, Z. Zhang, F. Yang, G. Nasti, B. Naydenov, W. C. Tsoi, Z. Li, X. Gao, Z. Wang, Y. Jia, E. Unger, M. Saliba, M. Li and A. Abate, *Science*, 2023, **379**, 399; https://doi.org/10.1126/science.add7331.
21 D. A. Jacobs, Y. Wu, H. Shen, C. Barugkin, F. J. Beck, T. P. White, K. Weber and K. R. Catchpole, *Phys. Chem. Chem. Phys.*, 2017, **19**, 3094; https://doi.org/10.1039/C6CP06989D.
22 J. Thiesbrummel, S. Shah, E. Gutierrez-Partida, F. Zu, F. Peña-Camargo, S. Zeiske, J. Diekmann, F. Ye, K. P. Peters, K. O. Brinkmann, P. Caprioglio, A. Dasgupta, S. Seo, F. A. Adeleye, J. Warby, Q. Jeangros, F. Lang, S. Zhang, S. Albrecht, T. Riedl, A. Armin, D. Neher, N. Koch, Y. Wu, V. M. Le Corre, H. Snaith and M. Stolterfoht, *Nat. Energy*, 2024, **9**, 664; https://doi.org/10.1038/s41560-024-01487-w.
23 E. Unger and T. J. Jacobsson, *ACS Energy Lett.*, 2022, **7**, 1240; https://doi.org/10.1021/acsenergylett.2c00330.
24 V. M. Le Corre, J. Diekmann, F. Peña-Camargo, J. Thiesbrummel, N. Tokmoldin, E. Gutierrez-Partida, K. P. Peters, L. Perdigón-Toro, M. H. Futscher, F. Lang, J. Warby, H. J. Snaith, D. Neher and M. Stolterfoht, *Sol. RRL*, 2022, **6**, 2100772; https://doi.org/10.1002/solr.202100772.
25 G. Y. Kim, A. Senocrate, T.-Y. Yang, G. Gregori, M. Grätzel and J. Maier, *Nat. Mater.*, 2018, **17**, 445; https://doi.org/10.1038/s41563-018-0038-0.
26 J. Li, Q. Dong, N. Li and L. Wang, *Adv. Energy Mater.*, 2017, **7**, 1602922; https://doi.org/10.1002/aenm.201602922.
27 A. K. Chauhan and P. Kumar, *J. Mater. Sci.: Mater. Electron.*, 2019, **30**, 9582; https://doi.org/10.1007/s10854-019-01292-2.

Received: 30th April 2025; Com. 25/7816